

High-Resolution Laser Spectroscopy on the Negative Osmium Ion

U. Warring,* M. Amoretti, C. Canali, A. Fischer, R. Heyne, J. O. Meier, Ch. Morhard, and A. Kellerbauer†

Max Planck Institute for Nuclear Physics, Saupfercheckweg 1, 69117 Heidelberg, Germany

(Received 5 October 2008; published 30 January 2009)

We have applied a combination of laser excitation and electric-field detachment to negative atomic ions for the first time, resulting in an enhancement of the excited-state detection efficiency for spectroscopy by at least 2 orders of magnitude. Applying the new method, a measurement of the bound-bound electric-dipole transition frequency in $^{192}\text{Os}^-$ was performed using collinear spectroscopy with a narrow-bandwidth cw laser. The transition frequency was found to be 257.831 190(35) THz [wavelength 1162.747 06(16) nm, wave number 8600.3227(12) cm^{-1}], in agreement with the only prior measurement, but with more than 100-fold higher precision.

DOI: 10.1103/PhysRevLett.102.043001

PACS numbers: 32.80.Gc, 32.30.Bv, 32.70.Cs, 37.10.Rs

Currently available techniques for the production of cold negative ions confined in ion traps are sympathetic cooling with light ions or electrons [1], buffer gas cooling [2,3], and resistive cooling [4]. They allow cooling to the temperature of the surrounding cryogenic environment, typically at 4 K if the apparatus itself is cooled with liquid helium. However, the achievable precision of spectroscopic investigations at these temperatures is still limited by inhomogeneous broadening, which could be reduced by further cooling the studied ions. Laser excitation of an electric-dipole transition in an atomic ion could be used to laser cool atomic anions to μK temperatures and use them to sympathetically cool other negative ions [5]. If demonstrated to work, this technique will allow the preparation of ultracold samples of any negative ion, ranging from elementary particles to molecular anions.

The potential experienced by the valence electron of a negative atomic ion is both shallow and short ranged [6]. Hence, in stark contrast to neutral atoms or positive ions, only a limited number of bound states (if any) are supported. Their binding energies are typically about an order of magnitude smaller than in atoms or positive ions. Bound excited states exist in only a minority of negative ions [7,8]. Among these, those cases where bound states of both odd and even parity are present are of particular interest. Since electric-dipole transitions between such states are allowed, they are amenable to experimental study using standard atomic-physics techniques, as well as to laser cooling.

Opposite-parity bound states have been predicted for the anions of some lanthanides and actinides [9–12] and for cesium [13–15], but for cesium and lanthanum their existence was later ruled out experimentally [16,17]. Some years ago, a survey of the negative osmium ion using infrared (IR) laser photodetachment spectroscopy (by two-photon absorption) with a pulsed dye laser led to the discovery of a strong resonant transition just below the photodetachment threshold [18]. This experimental evidence, combined with theoretical calculations on the ground state configuration [19], yields the energy level diagram shown in Fig. 1. The Os^- ion is the only presently

known anion that exhibits a bound excited state with opposite parity from the ground state. In the context of laser cooling, the resonant cross section of the transition and the excited-state lifetime are of major interest, because they determine the required laser power, the expected two-photon detachment loss rate, and the total cooling time.

In this Letter, we report on the results of high-resolution laser spectroscopy on the electric-dipole transition between the $4F^e$ ground and $6D^o$ bound excited states in the negative osmium ion. The experimental precision of the transition frequency was improved by more than 2 orders of magnitude, as compared with the only previous measurement. A high-precision determination of the transition frequency requires the use of a continuous-wave (cw) laser. While cw lasers yield narrower resonances and larger observed cross sections than pulsed lasers, they cannot deliver the high instantaneous intensities which characterize pulsed lasers. Therefore, we applied the technique of electric-field detachment (Ref. [8], Chap. 5), first conceived almost 50 years ago [20], to the laser-excited ions. In this way, the detection efficiency was increased by 2 orders of magnitude compared with two-photon detachment. Furthermore, we were able to measure the cross section of the transition directly, without resorting to theo-

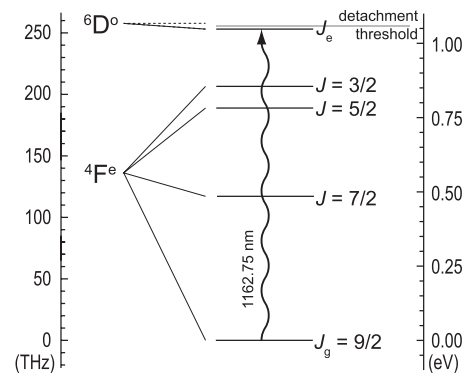


FIG. 1. Energy level diagram for $^{192}\text{Os}^-$. The wiggly arrow shows the explored transition from the $J_g = 9/2$ (ground) state to the J_e (excited) state.

retical models of the combined resonant and nonresonant processes.

The setup (see Fig. 2) with which the present measurements were performed is installed at the Max Planck Institute for Nuclear Physics (MPIK) in Heidelberg, Germany. The negative ions are produced with a Middleton-type sputter negative-ion source [21]. They are extracted and accelerated to form a beam whose energy can be set to $E = 2.5 \dots 6.5$ keV, before being mass-separated in a large ($R = 500$ mm) dipole magnet with a typical resolving power of 180. After the mass separation, the 50 nA ion beam consists of over 90% of $^{192}\text{Os}^-$, with low impurities of $^{190}\text{OsH}^-$ and $^{192}\text{OsH}^-$. An electrostatic bender guides the negative ions into the spectrometer section, which consists of an entrance diaphragm, a set of ionizing diaphragms, a deflector, a microchannel plate detector (MCP), and a Faraday cup. All diaphragms have a diameter of 7.5 mm, and the overall interaction region is 520 mm long. In the ionizer the beam passes a longitudinal electric field of up to 2×10^6 V m $^{-1}$. The ionizer is built as a sandwich of three apertures covered by copper meshes (transparency 70%). To the central aperture a voltage of up to ± 6.5 kV can be applied. A deflector leads the ions into a Faraday cup, at which 10% (5 nA) of the mass-separated beam typically arrive. In forward direction the MCP counts neutralized particles.

The light is produced by a cw optical parametric oscillator system custom-built for this experiment (Xiton Photonics), which is pumped by a frequency-doubled Nd:YAG laser. The pump beam at 532 nm wavelength is focused into a periodically poled lithium niobate crystal, which is embedded in a bow-tie cavity. The optical amplification yields a signal of 980 nm and an idler wave of 1163 nm fulfilling the quasi-phase-matching condition. The resonator oscillates on the idler wave, allowing roughly 4% of it to be coupled out and used for the experiment. The laser

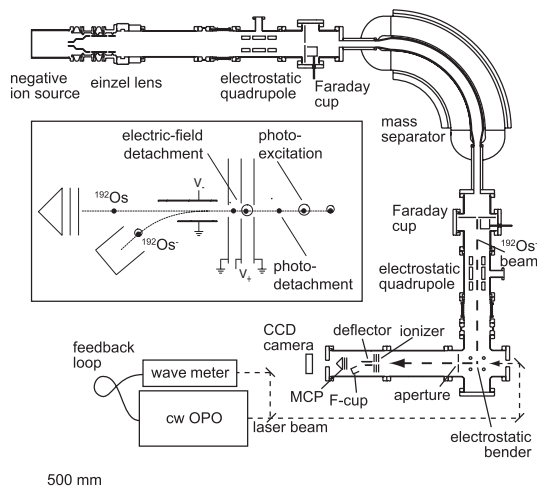


FIG. 2. Sketch of the experimental setup for the collinear laser spectroscopy. The inset is an enlarged sketch of the spectrometer section which illustrates the possible mechanisms for electron detachment.

beam has a bandwidth $\Gamma_{\text{las}} \leq 5$ MHz, and provides more than 170 mW of infrared light at a pumping power of 2 W.

The wavelength is determined and stabilized via a wave meter (HighFinesse WSU-30 IR), which is calibrated by a stabilized diode laser. The calibration laser is locked to the D_2 line in ^6Li via Doppler-free spectroscopy. Since the MCP can be moved out of the beam axis, the collimated laser beam (≈ 1 mm diameter) can be projected through the entire spectrometer arm and aligned with the help of a CCD camera (DAT TaperCamD). It is a well-known advantage of collinear spectroscopy that the effect of velocity bunching reduces the Doppler width of the resonance (see, for example, [22]). For our typical operating parameters, an ion temperature of $T \approx 1500$ K and an acceleration voltage of 5 kV, a reduction of about a factor of 10 with respect to the transverse case is achieved.

During data taking the optical parametric oscillator frequency can be swept continuously over a range of 1.5 GHz. For high-resolution measurements, the laser is scanned over a smaller region around the resonance. If an ion in the interaction zone is excited, it is either photodetached by a second photon, as in the work of Bilodeau and Haugen [18], or will be detached by the electric field of the ionizer (see inset of Fig. 2). Furthermore the excited state may be detached by other, competing mechanisms, of which the detachment by blackbody radiation was found to be the dominant one in measurements on Ca^- in a storage ring [23]. In any case the neutral atom will be detected by the MCP, with a detection efficiency of about 40%. Molecular contaminant ions will always be deflected onto the Faraday cup and not influence the MCP signal. In order to subtract background events, a chopper is introduced into the laser beam. Figure 3 shows a typical resonance recorded at 5 keV beam energy; it clearly shows the dramatic enhancement effect due to the ionizer. The peak width of $\Gamma_{\text{res}} = 45$ MHz is dominated by the Doppler width of the ion beam, and the shape is compatible with a Gaussian line profile except for an asymmetry, which is due to a corre-

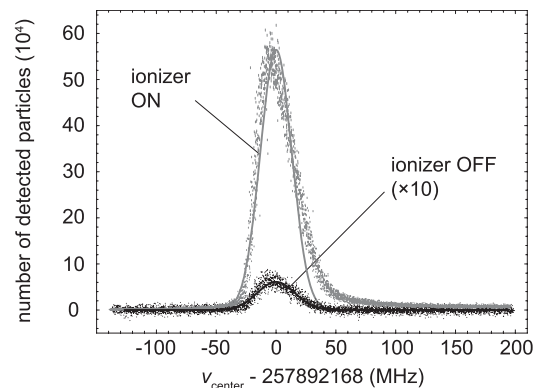


FIG. 3. Typical resonance of the dipole transition at an ion beam energy of 5 keV. The figure shows the efficiency gain due to the field-detachment process in comparison to all other detachment mechanisms. In addition, the corresponding Gaussian fits are shown as solid curves.

sponding asymmetry in the velocity distribution of the ions. This contributes a systematic uncertainty of 5 MHz to our frequency determination.

Since in a parallel collinear setup all measured frequencies are blueshifted, data points at different beam energies were taken (see Fig. 4) to extract the rest frame resonance frequency from fitting the data with the simple function for the Doppler shift $\nu = \nu_0 \sqrt{[c + v(E + \Delta E)]/[c - v(E + \Delta E)]}$. In addition to yielding the unshifted transition frequency ν_0 , the approach accommodates a possible offset of the beam energy ΔE , which was found from the fit to be 0.4(5) eV. The quality of the fit is illustrated by the residuals shown in Fig. 4(c). The resulting transition frequency $\nu_0 = 257.831\,190(35)$ THz is consistent with the previous experimental value of 257.8341(46) THz [18] (deviation 0.6σ), but more than 2 orders of magnitude more precise. The total uncertainty is limited by the frequency measurement with the wave meter, whose absolute accuracy is ± 30 MHz.

With the combination of laser excitation and field detachment, it is possible to measure the binding energy of the excited state directly. For this purpose, the laser was stabilized to the center of the resonance within 5 MHz and the electric field was scanned from 0 up to 2×10^6 V m⁻¹. Saturation of detached ions occurred at an electric field of 6×10^5 V m⁻¹. After modeling the resulting saturation data with a theoretical description for field detachment [24,25], the binding energy was extracted and found to be 11(2) meV, in agreement with, but less precise than, the indirect determination by laser photodetachment spectroscopy, which yielded 11.48(12) meV [18].

For a determination of the resonant cross section, it is useful to consider the time evolution of the ground and excited state populations in the beam, as well as the neutralized atoms, for different laser intensities, on resonance

and at constant ion beam energy. In order to describe the combined processes of photoexcitation and electric-field detachment of the excited state while also taking into account subsequent detachment, a system of standard rate equations is introduced:

$$\frac{dN_g(t)}{dt} = -\sigma_0 \phi N_g(t) + (\sigma_0 \phi + \tau_0^{-1}) N_e(t) \quad (1a)$$

$$\frac{dN_e(t)}{dt} = \sigma_0 \phi N_g(t) - (\sigma_0 \phi + \tau_0^{-1} + \sigma_d \phi + \tau_{\text{loss}}^{-1}) N_e(t) \quad (1b)$$

$$\frac{dN_d(t)}{dt} = (\sigma_d \phi + \tau_{\text{loss}}^{-1}) N_e(t), \quad (1c)$$

where N_g and N_e are the ground and excited state (later field-detached) populations and N_d is the number of detached atoms, respectively. τ_0 is the radiative lifetime of the excited (J_e) state into the ground (J_g) state which is related to the cross section σ_0 via

$$\tau_0 = c^2 / (4\pi^2 \sigma_0 \nu_0^2 \Gamma_{\text{res}}). \quad (2)$$

τ_{loss} denotes the lifetime of the excited state with respect to detachment processes other than absorption of a second laser photon, and ϕ is the laser-photon flux. In this model a possible decay into the intermediate ($J = 7/2$ and $5/2$) states is neglected because the partial lifetimes, which scale as ν^{-3} , are expected to be at least 8 times longer into those channels.

The set of differential equations (1a)–(1c) can be solved analytically and rearranged to express the populations $N_e(t)$ and $N_d(t)$ (where t is the time of flight of the ions within the laser beam) as a function of ϕ . The photon flux is modeled to have a spatial Gaussian profile, in line with observations from the beam profile CCD camera. Finally, the number of neutralized particles $N_{\text{neut}}(\sigma_0, \sigma_d, \tau_{\text{loss}}, N_0, P_{\text{las}}) = N_e(t) + N_d(t)$ is a function of the average laser power and has four independent parameters: The resonant and nonresonant cross sections σ_0 and σ_d , the number of ions within the overlap region N_0 , and the lifetime τ_{loss} . The latter was held fixed at the estimated blackbody radiation detachment rate, which was calculated to be $1/(5 \text{ ms})$ taking into account the known ionic resonance ≈ 3.6 meV above threshold [18]. The resulting cross sections σ_0 and σ_d are unaffected by this additional detachment channel even when allowing for detachment rates ($1/\tau_{\text{loss}}$) up to about a factor of 50 higher than our estimate. It is important to point out that this analysis does not rely on a precise knowledge of the MCP detection efficiency, provided it is constant during the course of the measurement. The function N_{neut} is very sensitive to the main parameter of interest, σ_0 , and N_0 , which corresponds to the asymptotic value of the function.

The number of neutral atoms detected on the MCP was recorded for beam energies ranging from 2.5 to 5.5 keV as a function of the laser intensity, which was varied via a polarizing beam splitter from 0 to 160 mW, without chang-

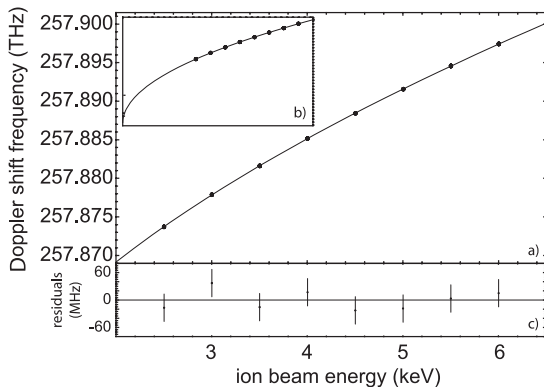


FIG. 4. (a) Blueshifted resonance frequencies as a function of the ion beam energy. The error bars are too small to be visible. The solid curve is the resulting fit for the Doppler shift. (b) For illustration the function is shown over the whole range (without explicit scales). (c) Residuals of the fit are shown to illustrate the fit quality.

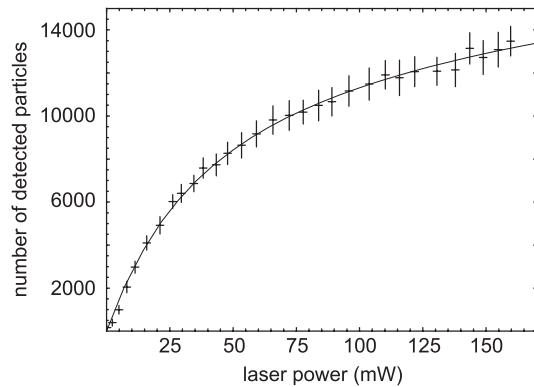


FIG. 5. Number of detected atoms versus laser intensity at the resonance frequency at a beam energy of $E = 2.5$ keV. The solid curve is a fit to the data according to Eqs. (1a)–(1c), which yields the cross section σ_0 for the transition.

ing other laser beam characteristics. Figure 5 shows a typical measurement at $E = 2.5$ keV, along with a fit according to the rate equation model. Ion-optical simulations have shown that the beam divergence between the diaphragms is 1.5° . This effectively reduces the interaction volume by 30%, but has otherwise no consequences for the parameters obtained from the fit. The weighted mean of ten such measurements yields a final value of $\sigma_0 = 2.5(7) \times 10^{-15}$ cm², where the uncertainty includes a contribution which is equal in magnitude to the beam divergence correction. While great care was taken to exclude other effects which can mimic the asymptotic behavior of the data, the MCP response, in particular, cannot be ruled out completely. Such an effect would make the cross section appear larger than the true value. The fit result does not constrain the photodetachment cross section very well, and only a rough estimate of $\sigma_d \approx 10^{-17}$ cm² was obtained, in line with the expected value for a nonresonant process. As pointed out above, the partial lifetime for decay to the ground state by spontaneous emission can be deduced from the cross section via Eq. (2), using $\Gamma_{\text{res}} = 45$ MHz, the experimental width of the resonance. In this way, a value of $\tau_0 = 3(1)$ ms was obtained.

The measured observed cross section and corresponding Einstein coefficient $A \approx 330$ s⁻¹ confirm that the resonance is due to an electric-dipole transition. The Einstein coefficient is, however, at the lower end of the scale for E1 transitions, but not unusual for a spin-forbidden resonance. Our measurements indicate that the natural linewidth is even narrower than suggested by the result of Bilodeau and Haugen, who found $A \approx 10^4$ s⁻¹ [18]. As concerns the prospect of laser cooling with this transition, the achievable Doppler temperature will in the foreseeable future be limited by the laser bandwidth. With our laser and at a detuning of $\delta = \Gamma_{\text{las}}/2$ the cooling rate may be as low as 50 Hz and cooling times from 80 K to the Doppler temperature prohibitively long. Therefore, precooling to liquid-helium temperature may be required, resulting in a cooling time of roughly 5 min.

In conclusion, the only known bound-bound transition between states of opposite parity in an atomic anion has been studied by high-resolution laser spectroscopy and its transition frequency determined to 10^{-7} precision. This is the most precise study of any atomic transition in negative ions. While the Einstein A coefficient of the relevant transition is lower than previously found, our work confirms that laser cooling of Os^- should be feasible.

This work was supported by the German Research Foundation (DFG) within the Emmy Noether program under Contract No. KE1369/1-1. We thank the MPIK accelerator group and workshop, in particular, M. König, V. Mallinger, and M. Beckmann. The assistance of the group of S. Jochim for the wave meter calibration is gratefully acknowledged. Finally, we are indebted to D. Beck (Michigan Technological University), R. C. Bilodeau (Lawrence Berkeley National Laboratory), H.-J. Kluge (Gesellschaft für Schwerionenforschung Darmstadt), and J. Walz (University of Mainz) for their comments on the manuscript.

*To whom correspondence should be addressed.

u.warring@mpi-hd.mpg.de

†a.kellerbauer@mpi-hd.mpg.de

- [1] G. Gabrielse *et al.*, Phys. Rev. Lett. **63**, 1360 (1989).
- [2] D. Gerlich, Phys. Scr. **T59**, 256 (1995).
- [3] Y. Liu *et al.*, in *Proceedings of the 19th Particle Accelerator Conference, Chicago, 2001* (IEEE, Piscataway, NJ, 2001), Vol. 5, p. 3885.
- [4] G. Gabrielse *et al.*, Phys. Rev. Lett. **82**, 3198 (1999).
- [5] A. Kellerbauer and J. Walz, New J. Phys. **8**, 45 (2006).
- [6] D. J. Pegg, Rep. Prog. Phys. **67**, 857 (2004).
- [7] T. Andersen, H. K. Haugen, and H. Hotop, J. Phys. Chem. Ref. Data **28**, 1511 (1999).
- [8] T. Andersen, Phys. Rep. **394**, 157 (2004).
- [9] S. Vosko *et al.*, Phys. Rev. A **43**, 6389 (1991).
- [10] D. Datta and D. R. Beck, Phys. Rev. A **50**, 1107 (1994).
- [11] K. Dinov *et al.*, Phys. Rev. A **50**, 1144 (1994).
- [12] S. M. O'Malley and D. R. Beck, Phys. Rev. A **78**, 012510 (2008).
- [13] C. H. Greene, Phys. Rev. A **42**, 1405 (1990).
- [14] J. L. Krause and R. S. Berry, Comments At. Mol. Phys. **18**, 91 (1986).
- [15] C. Froese Fischer and D. Chen, THEOCHEM **199**, 61 (1989).
- [16] A. M. Covington *et al.*, J. Phys. B **31**, L855 (1998).
- [17] M. Scheer *et al.*, Phys. Rev. Lett. **80**, 684 (1998).
- [18] R. C. Bilodeau and H. K. Haugen, Phys. Rev. Lett. **85**, 534 (2000).
- [19] P. Norquist and D. Beck, Phys. Rev. A **61**, 014501 (1999).
- [20] A. C. Riviere and D. R. Sweetman, Phys. Rev. Lett. **5**, 560 (1960).
- [21] R. Middleton, Nucl. Instrum. Methods **214**, 139 (1983).
- [22] W. Demtröder, *Laser Spectroscopy* (Springer, Berlin, 2002), 3rd ed., p. 553.
- [23] H. K. Haugen *et al.*, Phys. Rev. A **46**, R1 (1992).
- [24] B. M. Smirnov and M. I. Chibisov, Sov. Phys. JETP **22**, 585 (1966).
- [25] A. M. Perelomov *et al.*, Sov. Phys. JETP **23**, 924 (1966).